Journal of Theoretical and Applied Information Technology
31st May 2022. Vol.100. No 10

ISSN: 1992-8645 www.jatit.org E-ISSN: 1817-3195

IMPLEMENTATION OF PMBLDC MOTOR DRIVEN ELECTRIC VEHICLE POWERED BY SOLAR

M.V. RAMESH[1], RAVI KUMAR MELIMI[2], T.SRINIVASA RAO[3], P.MUTHU KUMAR[4]

[1,4]Associate Professor, Department of Electrical & Electronics Engineering,

Prasad V. Potluri Siddhartha Institute of Technology, Vijayawada, Andhra Pradesh, India.

[2,3] Assistant Professor, Department of Electrical & Electronics Engineering,

Prasad V. Potluri Siddhartha Institute of Technology, Vijayawada, Andhra Pradesh, India.

E-mail: [1]vrameshmaddukuri@gmail.com, [2]ravikumar.melimi@gmail.com, [3]srinuthumati@gmail.com and [4]muthukumarvlsi@gmail.com

ABSTRACT

In the recent years the awareness on the global warming effect leads to the interest in development of electric vehicle technology for all the stakeholders. The technology is growing rapidly. With more concern on our environment Solar PV system being introduced. The aim of the paper is the application of solar PV system to electric vehicle along with its design aspects. The driven system to the electric vehicle is through PMBLDC motor. PMBLDC motor input is taken from battery bank. The battery bank is employed for the storage of the power. The power produced by the PV system is transmitted through MPPT charge controller, battery bank and PMBLDC motor. The designed Electric Vehicle is tested and validated successfully.

Keywords: *Solar PV system; MPPT, Battery bank, PMBLDC motor, Electric Vehicle*

1. INTRODUCTION

Due to numerous conventional vehicles the pollution in the environment is increasing day by day. This can be reduced by the usage of electric vehicles [9].The electric vehicles are comfortable in the future for road transportation that can be used more effectively and efficiently by reducing the oil consumption and gas emission [1]. Permanent Magnet Brushless DC motor (PMBLDC) motor is mostly employed in electrical vehicle because to its high efficiency and torque [3][4]. It also works well with dynamic load and varied set points. It is a three phase permanent magnet synchronous motor with trapezoidal EMF which requires DC supply [5][13].

The battery energy storage system integrates intermittent solar energy to grid [2]. The peak power demand of the electric vehicle can be met with the battery having high power density. The most of the electrical power is generated by using fossil fuels that result in emissions of huge carbon into the atmosphere. This is the reason for the electrical engineers to use renewable energy sources. An extensive research work for increasing the efficiency of solar cell is going on [3].For the improvement of the performance of overall PV system, solar charge controller is needed to protect the storage batteries [6].

For increasing the efficiency and obtaining the maximum power from panel, MPPT controller plays a major role [14]. The boost converter fed sensorless position control of PMBLDC motor drive has been implemented in flour mill application for power factor correction [10]. In [11] sensorless position control of PMBLDC motor is implemented in phase band commutation signal generation from the line voltages.

The paper organized as follows. Mechanical design aspects like load calculation, chassis design and BLDC motor drive system are presented in section 2. The Storage system to power the Electric Vehicle is mentioned in Section 3. The MPPT charge controller to extract maximum solar power is presented in Section 4. The description of Solar PV system to generate the power to drive the motor is presented in Section 5. The fabrication of the proposed system is presented in Section 6. The Conclusions is presented in Section 7.

Journal of Theoretical and Applied Information Technology
31st May 2022. Vol.100. No 10

ISSN: 1992-8645 www.jatit.org E-ISSN: 1817-3195

2. MECHANICAL DESIGN ASPECTS

2.1. Load Designs

Assuming BLDC motor with speed 3000rpm, power 3kW and velocity 30km/hr, the load of the Electrical Vehicle is estimated,

$$T_m = \frac{60*P}{2\pi*3000} \quad (1)$$

Velocity, $V = r*\omega_m$ (2)

r (radius of wheel) = 15cm

ω_a = axle speed

$$\omega_a = \frac{2*\pi*N}{60} \quad (3)$$

$$\text{Force } F = \frac{T}{R_x} \quad (4)$$

$$\text{Weight, } W = \frac{F}{\mu} \quad (5)$$

Rolling friction in between tire and road is assumed as 0.02

Force without torque loss,

$$F = \frac{T}{R_x} \quad (6)$$

$$\text{Weight (w)} = \frac{F}{\mu} \quad (7)$$

The calculations are prepared for 25%, 20% and 10% torque loss.

I & C type chassis was modelled using pro-e wildfire 2.0 and the stress analysis is made using ANSYS. The Chassis is modeled similar to TATA ACE measurements. The following chassis values are considered as, Total length = 300 cm Total width =130 cm and chassis has five crosses and three lateral members [5].

The meshing, load and boundary conditions, stress intensity are to be considered while designing the chassis.

These day's C-type is used in many automobile chassis. Structural analysis is made using ANSYS for C section chassis.

Based on the measurements, the chassis was designed in pro-e software and shown in Figure 1.

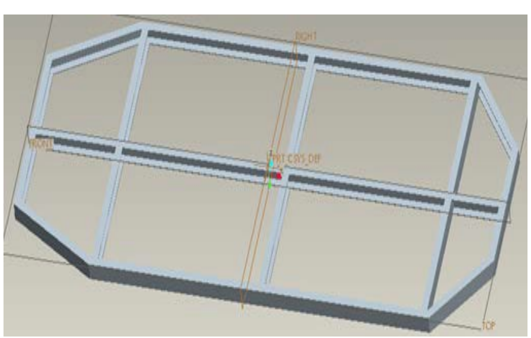

Figure 1: Chassis Design in PRO-E

The value of von mises stresses for C type chassis is 58.60 MPa and shown in Figure 2[8].

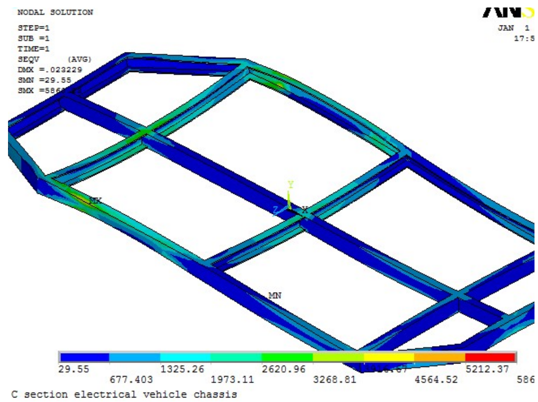

Figure 2: C-Type Cross Section Von Mises Stresses

On comparing C-type with I-type sections, it is found C-type is better in terms of von mises stresses, deformation, manufacturing cost and strength of the chassis.

Results are presented in table 1, under the pressure load 1.73N/cm2, young's modulus 130MPa, poison's ratio between 0.2-0.3 and density 0.0078N/cm^3 for CS iron material. Based on calculations the chassis is fabricated with C-type and CS iron.

Table 1: Comparison for C-type Chassis.

S. No.	Cross Section Type	Intensity of stress	Von Mises Stresses	Total Deformation
1.	I-type	65.2	58.9	1.538 x10^{-4}
2.	C-type	62.6	58.6	1.676 x 10^{-4}

a. Drive System

The drive system consists of BLDC motor, Gear Box, Universal joint transmission, Differential Assembly and Wheels.

PMBLDC motor is a synchronous motor with rotor of permanent magnets and wound stator poles are wire wound.

Permanent magnets are made of Ferrite material. These days, rare-earth alloy magnets gaining importance [9].

To rotate the motor, stator windings energized need to be in order. To energize the stator winding,

ISSN: 1992-8645 www.jatit.org E-ISSN: 1817-3195

the rotor position is to be known and should follow the energizing sequence. Hall Effect sensors are used to perceive the Rotor position which embedded in the stator. The circuit diagram of PMBLDC motor shown in Figure 3. The constructional view of the motor shown in Figure 4.

The motor specifications are,

Voltage - 48V, Power - 3kWatts, Speed – 3000rpm

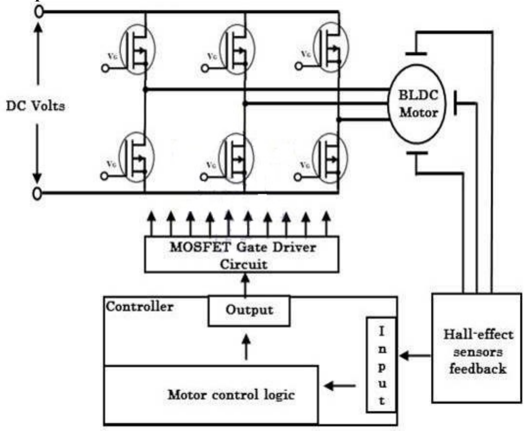

Figure 3: Circuit Diagram of BLDC Motor

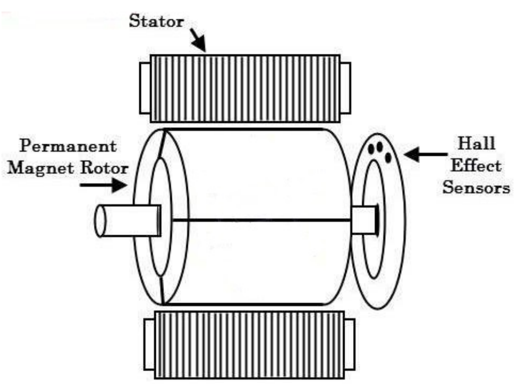

Figure 4: Constructional View of the BLDC Motor

The 3 phases back EMF waveform is shown in Figure. 5.

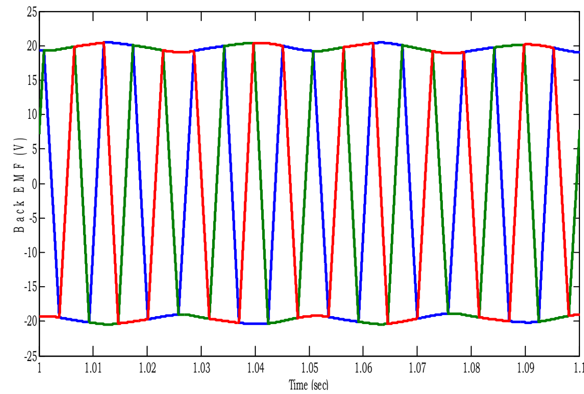

Figure 5: Three Phase Back Emf of BLDC Motor with Respect To Time

The Speed – Torque Characteristics of BLDC motor is shown in Figure. 6.

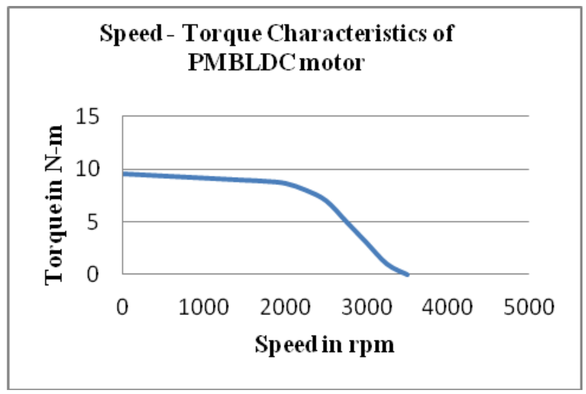

Figure 6: PMBLDC Motor Speed Torque Characteristics

The graph between the Speed and the Duty Ratio is shown in Figure 7.

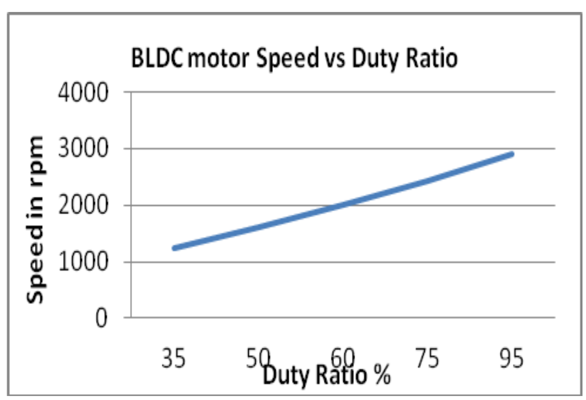

Figure 7: BLDC Motor Speed with respect to Duty Ratio

A gear box converts the shaft speed. The torque is also changed with this device. These have the interlocking teeth that mesh each other and can be in the form of wheel.

Universal joint allows the angle to change between connected parts with certain range. The various parts is installed and connected to frame [10].

3. STORAGE SYSTEM

Various types of batteries like Lead Acid, Lithium Ion, Molten Salt, Nickel Metal Hydride and Lithium Sulphur are available for powering the Electric Vehicle. Important characteristics like safety, storage efficiency, constructive characteristics, life cycles and price are to be considered. Lead acid battery is most commonly used for electric vehicles. Lead Acid battery equivalent circuit is implemented using MATLAB/SIMULINK.

The battery system equivalent circuit shown in Figure 8.

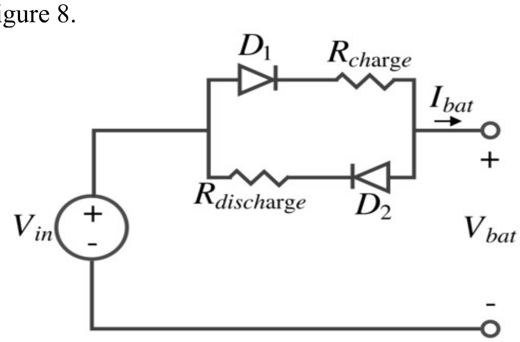

Figure 8: Battery Equivalent Circuit

$$V_b = E_{on} - K_p \frac{Q_b}{Q_b - it} it - K_p \frac{Q_b}{Q_b - it} i - R_b \cdot i + C \quad (8)$$

$$V_b = E_{on} - K_p \frac{Q_b}{Q_b - it} it - K_p \frac{Q_b}{it - 0.1Q_b} i - R_b \cdot i + C \quad (9)$$

Where,

V_b: Battery Voltage, V;

E_{on}: Nominal voltage, V;

K_p: Polarization Resistance, Ω;

Q_b: Battery capacity, Ah;

R_b: Battery Internal Resistance, Ω;

C: Exponential Voltage, V;

4. SOLAR CHARGE CONTROLLER

Buck Boost converter is used to regulate the voltage across the battery. The battery system voltage is 48V. The Solar PV system voltage varies from 0 to 61V. The charge controls the voltage and makes the battery voltage to be 48V (nearly). In order to achieve the constant voltage, the duty cycle of the converter has to be varied accordingly. The variation of this duty cycle is attained using MPPT algorithm. The effectiveness of the converter depends upon the sturdiness of the algorithm. The circuit diagram of Buck Boost converter shown in Figure 9.

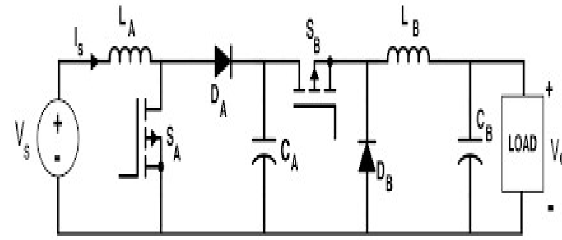

Figure 9: The Buck-Boost Converter Circuit

The mathematical expression for Buck Boost converter is as follows. The duty cycle is used to obtain the required voltage.

$$V_o = \frac{V_{in}}{1-D} \quad (10)$$

$$L_{inv} = \frac{V_{in} * (V_o - V_{in})}{\Delta I_L * f_c * V_o} \quad (11)$$

$$C_{inv} = \frac{D * V_o}{f_c * R * \Delta V_o} \quad (12)$$

Where,

V_o: Converter Output voltage,

V_{in}: Input voltage of the converter

L_{inv}: Inductance of the Inverter and

C_{inv} : Capacitance of the Inverter;

D: Duty cycle of the converter;

f_s: Switching frequency;

ΔI_L: Inductor ripple current;

ΔV_o: Output ripple voltage

Maximum Power Point Tracking (MPPT) is utilized in wind generators and PV structures to upgrade power extraction regarding all conditions. While the proportion of daylight differs, the load characteristics that gives the maximum power transfer efficiency changes, with that the effectiveness of the system is improved while the load characteristics adjustment to keep up the power exchange at the most basic efficiency. This load characteristic is known as maximum power point (MPP) and MPPT is the technique of discovering this point and maintaining the load characteristic there.

Different approaches the maximization of solar array o/p power of developed through controllers. The effective distinguished instruction set is developed by MPPT's and improve including them based entirely on the working circumstances of the array.

1. P&O (Perturb and Observe) Technique
2. Constant Voltage Method
3. Current Sweep
4. Incremental Conductance Method

Journal of Theoretical and Applied Information Technology
31st May 2022. Vol.100. No 10

ISSN: 1992-8645 www.jatit.org E-ISSN: 1817-3195

P&O approach have the counteractive action is to track the utmost power under the quick differentiating climatic condition is changed by the IC scheme. The P&O is the simpler for strategy than INC to the quality of execution in any case with startlingly fluctuating climatic conditions; P&O holds restrictions moreover may not work accurately on some occurrences. Consequently, changed INC (variable step equal to the slop dP/dV) is considered.

This changed MPPT development limits the tracking with time range when appeared from normal INC MPPT. Based on this case the INC has a slope of the Photo Voltaic array characteristics is positive toward left of MPP and 0 at MPP, the right of MPP is negative. The flowchart of INC is mentioned in Figure 10.

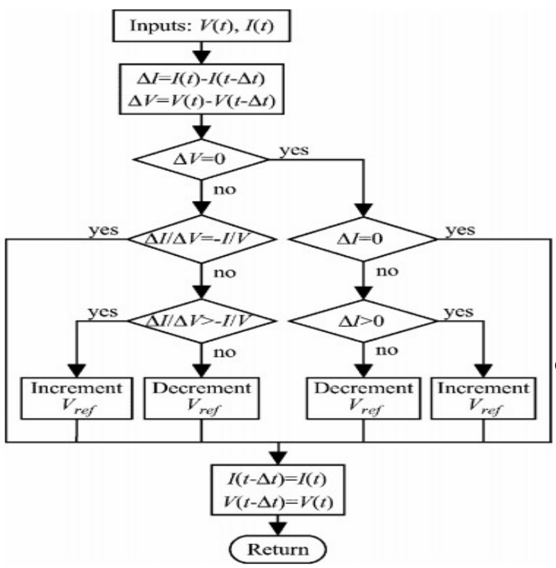

Figure 10: The Flowchart of INC

5. SOLAR PV SYSTEM

Solar PV cell is major innovation technically in lifetime and changing the way we use our energy needs now and in future.

Most commercially used solar PV systems uses silicon PV cells because of its cost and efficiency.

Both mono-crystalline and poly-crystalline panels are manufactured from silicon into mold to form polycrystalline panel.

The equivalent circuit of Solar PV cell shown in Figure 11.

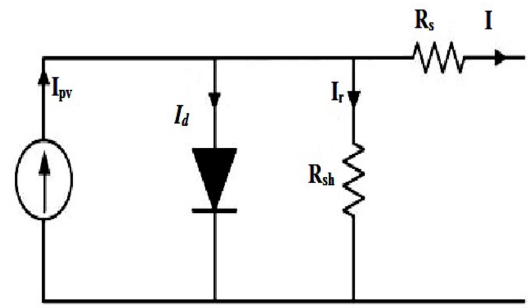

Figure 11: PV Cell Equivalent Diode Model

$$I_{pv} = I_{lg} - I_{opv} * \left[exp\left\{q * \frac{V_{pv} + I_{pv} * R_{se}}{A * k * T_c}\right\} - 1\right] - \frac{V_{pv} + I_{pv} * R_{se}}{R_{sh}} \quad (13)$$

$$I_{opv} = I_{or} * \left(\frac{T_c}{T_{ref}}\right)^3 * \left[exp\left\{q * E_{gs} * \frac{\frac{1}{T_{ref}} - \frac{1}{T_c}}{A * K}\right\}\right] \quad (14)$$

$$I_{lg} = \{I_{sc} + K_i * (T_c - 25)\} * \lambda \quad (15)$$

$$I_{pv} = N_p * I_{lg} - N_p - I_{opv} * \left[exp\left\{q * \frac{V_{pv} + I_{pv} * R_{se}}{A * k * T_c}\right\} - 1\right] - \frac{V_{pv} * \left(\frac{N_p}{N_s}\right) + I_{pv} * R_{se}}{R_{sh}} \quad (16)$$

Where,

I_{pv}&V_{pv} : Photovoltaic cell output voltage and current;

I_{opv} : Reverse-saturation current of PV cell;

T_c : Solar cell temperature;

k : Boltzmann's constant @ 1.38*10^{-19} J/K;

q : Electron charge @ 1.6*10^{-23} C;

K_i: SC current coefficient of temperature at I_{sc};

λ : Solar cell irradiation, W/m^2;

I_{sc}: SC current at 25° Celsius;

I_{lg}: Light generated current;

E_{gs}: Silicon Band gap;

A: Ideality factor;

T_{ref}: Temperature Reference;

I_{or}: Saturation current of Cell, T_{ref};

R_{sh}: Parallel Resistance;

R_{se}: Series Resistance;

Average day time temperature of the available PV solar panel at the installed location is shown in Figure 12.

ISSN: 1992-8645 www.jatit.org E-ISSN: 1817-3195

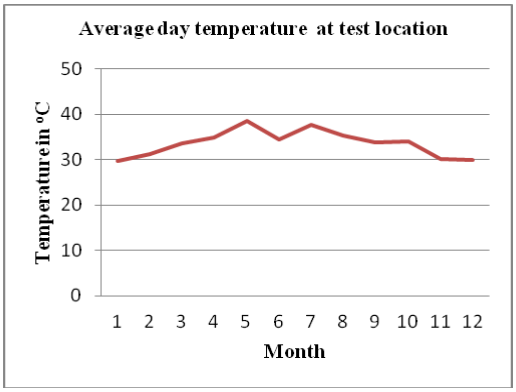

Figure 12: Average Day Time Temperature at the Test Location

The Solar Irradiance at test location is shown in Figure 13.

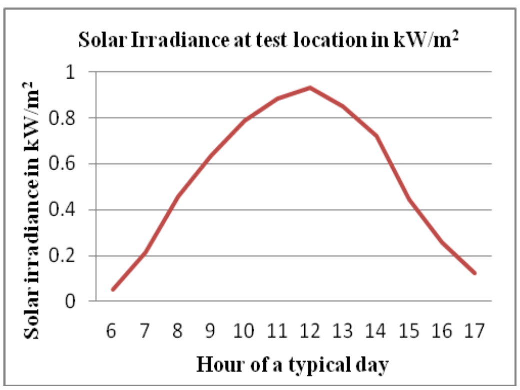

Figure 13: Hourly Solar Irradiance at Given Test Location for a Typical Day

The VI characteristic of Solar Panel is shown in Figure 14.

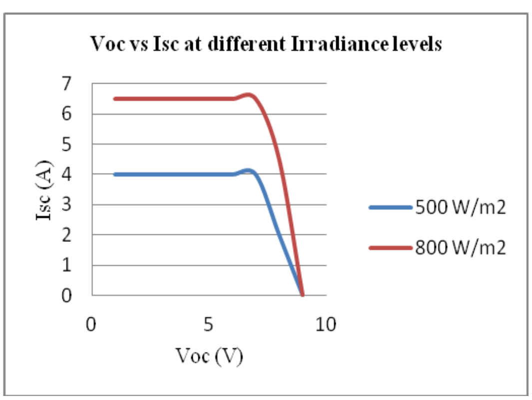

Figure 14: V-I Characteristics of the Solar Panel at Different Irradiance

The hourly power output curve of PV panel is shown in Figure 15.

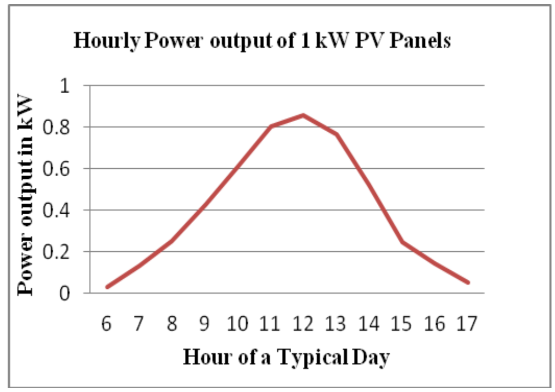

Figure 15: Hourly Power Output of 1kW PV Panel

$$f_{roll} = f_r * M * g \quad (17)$$

$$f_{AD} = \frac{1}{2} * \xi * C_D * A * V^2 \quad (18)$$

$$f_{grade} = M * g * sin\alpha \quad (19)$$

$$f_{acc} = M * a = M * \frac{dV}{dt} \quad (20)$$

$$T_{wheel} = F_{tot} * R_{wheel} + I_{wheel} * \frac{d\omega_{wheel}}{dt} + T_{loss} \quad (21)$$

$$\omega_{wheel} = \frac{v}{R_{wheel}}(s+1) \quad (22)$$

6. FABRICATION

The fabricated C-type chassis with rear axle assembly is shown in Figure 16.

Figure 16: Chassis with rear assembly

The chassis mounted with BLDC motor and Gear box is as shown in Figure 17.

Figure 17: Design with Chassis, Rear Assembly & Motor with Gear Box

The complete Solar based BLDC motor driven Electric Vehicle is as shown in Figure 18.

Figure 18: Completed Vehicle

Specifications:

S. No	Name of the item	Details
1	C-type chassis	
2	BLDC motor	3kW, 48V, 3000rpm
3	Gear box	1:15 ratio, unit 3
4	Battery	Lead acid, 48V, 100AH, deep cycle rechargeable battery
5	Charge controller	48V, 20A
6	Solar PV module	4 units Rated Power – 315W_p V_{mp} – 36.92V I_{mp} – 8.55A V_{oc} – 46.15V I_{sc} – 8.91A Series Fuse Rating – 15A Diode Rating – 15A

7. CONCLUSION

In this paper design and fabrication of solar based electric vehicle is proposed. PMBLDC motor driven is provided to drive the vehicle. The solar PV panels erected on top of electric vehicle, and the MPPT charge controller connected to stable solar power. The battery bank is installed for storing the power generated by the solar PV system. The power input to motor is acquired from battery bank.

At test location Vijayawada having latitude 16.5ºN, the maximum available solar irradiance is found to be 750W/m^2. The average sunny hours at the test location is 4.5 hours. The installed 1kW solar module generates about 4.5kWh energy. The battery can be charged in 1 day with the configured Solar PV system. BLDC installed is able to drive a load of 1.5 ton capacity at a speed of 40kmph. With this design zero emission free environments can be achieved.

REFERENCES

[1] Chunhua Liu, K. T. Chau, Diyun Wu, ShuangGao "Opportunities and Challenges of Vehicle-to-Home, Vehicle-to-Vehicle, and Vehicle-to-Grid Technologies" IEEE, Vol: 101 , Issue: 11 , pp. 2409-2427, Nov. 2013.

[2] Yutaka Ota, Haruhito Taniguchi, Tatsuhito Nakajima, Kithsiri M. Liyanage, JumpeiBaba, and Akihiko Yokoyama "Autonomous Distributed V2G (Vehicle-to-Grid) Satisfying Scheduled Charging", IEEE

TRANSACTIONS ON SMART GRID, Vol. 3, No. 1, pp. 559, March 2012.

[3] V.V. Tyagia, Nurul A.A. Rahim, N.A. Rahim , Jeyraj A./L. Selvaraj "Progress in solar PV technology" Research and achievement", ELSEVIER, pp 444-454, September 2012.

[4] C. Gnanavel, T. Baldwin Immanuel, P. Muthukumar, and Padma Suresh Lekshmi Kanthan, "Investigation on Four Quadrant Operation of BLDC MOTOR Using Spartan-6 FPGA", Springer Nature Singapore, ICSCS 2018, CCIS 837, (2018pp. 752–763, 2018pp.1-12.

[5] N. Veeramuthulingam, A. Ezhilarasi, M. Ramaswamy, P. Muthukumar,"Modeling of Brushless DC Motor Using Adaptive Control", Springer, Soft Computing Systems. ICSCS 2018. Communications in Computer and Information Science, vol. 837, pp. 764-775, 2018.

[6] HMasheleniaX.FCarelseb "Microcontroller-based charge controller for stand-alone photovoltaic systems", Vol. 61, Issue 4, pp. 225-230, October 1997.

[7] Sk.Bala Saidulu, G.Vijay Kumar G.Diwakar, M.V.Ramesh, "Design and Fabrication of Chassis For Electrical Vehicle" International Journal of Advanced Research in Engineering & Management (IJAREM) Volume 02, Issue 01, January 2016.

[8] M. V. Ramesh, B. Mohan and M. Seshu, 2018, "Solar Based Electrical Vehicle System", International Journal for Research in Engineering Application & Management, 2018, pp 423-428.

[9] M.V.Ramesh, J.Amarnath, S.Kamakshaiah, B.Jawaharlal and Gorantla.S.Rao "Speed Torque Characteristics of Brushless DC Motor in either direction on load using ARM Controller" Journal of Energy Technologies and Policy, IISTE, Vol. 2, No. 1, 2011, pp 37-48, Impact factor: 6, ISSN 2225-0573.

[10] C.Veeranjaneyulu, U. Hari Babu, "Design and Structural Analysis of Differential Gear Box at Different Loads", International Journal of Advanced Engineering Research and Studies, Vol. I, Issue II, January-March, 2012, pp 65-69.

[11] S. Manglik, A. Sen, B. Singh and B. K. Panigrahi, "Low Power Sensorless PMBLDC Motor Drive with PFC for Domestic Flour Mill," 2020 3rd International Conference on Energy, Power and Environment: Towards Clean Energy Technologies, 2021, pp. 1-5, doi: 10.1109/ICEPE50861.2021.9404433.

[12] S. Singh, S. Kumar, U. K. Kalla and S. Singh, "Reduced Sensor PMBLDC Motor Drive with Power Factor Correction and Speed Control," 2020 International Conference on Power Electronics and Renewable Energy Applications (PEREA), 2020, pp. 1-6, doi: 10.1109/PEREA51218.2020.9339778.

[13] Hanif F. Prasetyo, Arief S. Rohman, Farkhad I. Hariadi, HilwadiHindersah "Controls of BLDC motors in electric vehicle Testing Simulator", 2016 6th International Conference on System Engineering and Technology (ICSET)IEEE, 3-4 Oct. 2016, Bandung, Indonesia.

[14] DoggaRaveendhra, Babloo Kumar, Devesh Mishra, MeenakshiMankotia "Design of FPGA based open circuit voltage MPPT charge controller for solar PV system", 2013 International Conference on Circuits, Power and Computing Technologies (ICCPCT)IEEE, 20-21 March 2013, Nagercoil, India.